Long Non-Coding RNA MIR4435-2HG Promotes Glycolysis and Tumor Immunity in Pancreatic Cancer Through Absorption of microRNA-582-5p to Target GPX8

Huimin Lu
Sichuan University West China Hospital
Mao Li
Sichuan University West China Hospital
Dujiang Yang
Sichuan University West China Hospital
Zhenlu Li
Sichuan University West China Hospital
Chao Yue
Sichuan University West China Hospital
Jiafan Song
Sichuan University West China Hospital
Xing Wang
Sichuan University West China Hospital
Weiming Hu (Huweiming365@163.com)
Sichuan University West China Hospital

Research Article

Keywords: Pancreatic cancer, Long non-coding RNA MIR4435-2HG, MicroRNA-582-5p, Glutathione peroxidase-8, Glycolysis, Tumor immunity, Growth

Posted Date: December 8th, 2021

DOI: https://doi.org/10.21203/rs.3.rs-1112369/v1

Abstract

Objective

Long non-coding RNA MIR4435-2HG (MIR4435-2HG) has been clarified as a promoter in cancers, but its involvement in pancreatic cancer (PC) was not thoroughly probed.

Methods

MIR4435-2HG levels in PC clinical tissue and cell lines were analyzed. The relation between MIR4435-2HG levels with clinicopathological characteristics and survival of PC patients was evaluated. After transfection with plasmids altering MIR4435-2HG, microRNA (miR)-582-5p or glutathione peroxidase-8 (GPX8), the biological functions, glycolysis and tumor immunity of PANC-1 cells were observed. *In vivo* tumor growth was observed in nude mice.

Results

MIR4435-2HG was highly expressed in PC tissues and cell lines which was negatively correlated with clinicopathological characteristics and prognosis of PC patients. MIR4435-2HG or GPX8 inhibition or miR-582-5p elevation restrained the growth, glycolysis and immunity of PANC-1 cells. miR-582-5p down-regulation or GPX8 up-regulation reversed the effect of silenced MIR4435-2HG on PANC-1 cells. *In vivo* experiments further confirmed the *in vitro* results.

Conclusion

Our study highlights that MIR4435-2HG promotes glycolysis and tumor immunity in PC through absorption of micR-582-5p to target GPX8.

Introduction

About 86023 pancreatic cancer (PC) cases were diagnosed in China in 2020, with an estimated age-standardized incidence rate of 3.9%. Early PC is usually clinically asymptomatic, and the disease becomes obvious only after the tumor invades or metastasizes. Typical symptoms include abdominal pain or middle back pain, weight loss and obstructive jaundice [1]. People with any risk factors such as smoking, obesity, genetics, diabetes, diet, inactivity are at higher risk of PC [2]. Methods used to diagnose PC include ultrasonography, EUS, CT, MR, endoscopic retrograde cholangiopancreatography, and thin needle aspiration [3]. Unfortunately, the cure rate of PC is only 9%, and if without treatment, the median survival of patients with metastatic PC is only 3 months [4]. In respect to effective treatments of PC, huge efforts are largely required to decipher the molecular mechanism of the disease.

Long noncoding RNA (lncRNA) has undergone significant changes in the progression of cancer. In particular, lncRNAs exert multiple functions in PC and have valuable implications in the progression of PC [5]. Studies have listed various lncRNAs that could mediate metabolic reprogramming of PC cells. For instance, LncRNA plasmacytoma variant translocation 1 [6] and MACC1 antisense RNA 1 [7] could repress the progression of PC through impeding glycolysis of cancer cells. Regarding to MIR4435-2HG, it has been corroborated that MIR4435-2HG enhances metastatic activity of gastric cancer (GC) cells [8] and lung cancer cells [9], while MIR4435-2HG-oriented mechanism in PC was insufficiently studied. LncRNA can be used as a miRNA decoy to regulate gene expression, and any disruption of the regulatory loop may ultimately lead to cancer initiation and development [10]. In a varied range of cancers, miR-582-5p is usually found to act suppressively to decrease the malignant behaviors of cancer cells. Tian Y *et al*. have concluded that miR-582-5p obstructs bone metastasis of prostate cancer cells [11], while Liu J *et al*. have discovered the inhibitory impacts of miR-582-5p on non-small cell lung cancer (NSCLC) cells [12]. Glutathione peroxidases (GPXs) could reduce the damage associated with intracellular oxidative stress and have been found to be closely related to tumorigenesis [13]. As a non-selenium congener of GPXs family, GPX8 has become a key player in biological environments, far beyond the detoxification of hydroperoxides [14]. Indeed, GPX8 serves essentially for regulating aggressive breast cancer [15] and predicting prognosis of GC [16]. With regard to MIR4435-2HG-mediated miR-582-5p/GPX8 network in PC, little few research has been initiated. Innovatively, our research was implemented to unveil the action of MIR4435-2HG/miR-582-5p/GPX8 axis as to the aspects of growth, glycolysis and immunity of PC cells.

Methods And Materials

Ethics statement

The study was approved by the committee of West China Hospital of Sichuan University, and all subjects had signed a written consent form. Animal treatments were processed in coincidence with Animal Care and Use Guidelines of Animal Ethic Committee in West China Hospital of Sichuan University.

Clinical samples

Ninety-six PC patients were enrolled, and cancer tissue and normal tissues were surgically obtained. Patients were confirmed as PC through the WHO standard histopathological diagnosis. No radiotherapy or chemotherapy was performed before and after the operation. After the operation, the patients were followed up every six months by outpatient reviews, and the median follow-up was 60 months.

Cell culture

PC cell lines AsPC-1 (CRL-1682), BxPC-3 (CRL-1687), PANC-1 (CRL-1469), MIA PaCa-2 (CRM-CRL-1420) and SW1990 (CRL-2172), and human pancreatic duct epithelial cell line hTERT-HPNE (CRL-4023) were obtained from ATCC (CA, USA). AsPC-1 and BxPC-3 cells were cultured with Roswell Park Memorial Institute 1640 medium (A4192301), PANC-1 and MIA PaCa-2 cells in Dulbecco's Modified Eagle Medium (DMEM; A4192101) while SW1990 cells in L-15 medium (11415114). The above medium was added with

10% fetal bovine serum (FBS; 16140063). hTERT-HPNE cells were placed in complete growth medium. All media were purchased from Gibco (CA, USA) [17].

Cell transfection

PANC-1 cells with 40-50% confluence were subjected to transfection with plasmids (GenePharma, Shanghai, China) through Lipofectamine® 2000 (11668019; Invitrogen, CA, USA). The plasmids were transfected alone or in combination as following: small interfering RNA (si)-negative control (NC), si-MIR4435-2HG, mimic-NC, mimic-miR-582-5p, short hairpin RNA (sh)-NC, sh-GPX8, si-MIR4435-2HG + inhibitor-NC, si-MIR4435-2HG + inhibitor-miR-582-5p, si-MIR4435-2HG + overexpressed (oe)-NC, si-MIR4435-2HG + oe-GPX8. At 48 h post transfection, cells were amassed [18].

Cell counting kit (CCK)-8 assay

Using the CCK-8 kit (CK04; Dojindo, Kumamoto, Japan), cell proliferation was tested. Cells (4000 cells/well) were added with CCK-8 reagent (200 μL) at 0, 24, 48, 72, and 96 h, respectively, and incubated to detect absorbance on a microplate reader at 450 nm [19].

Colony formation assay

Cells were cultured in 10% FBS-DMEM and cultured for 2 w at 1×10^3 cells/well. Then, cell colonies that were fixed in 10% formaldehyde (252549; Sigma-Aldrich, CA, USA) were stained with 0.1% crystal violet (C0775; Sigma-Aldrich) and counted by a microscope (Olympus, Tokyo, Japan) [20].

Scratch test

Cells with 80-90% confluence were wounded by a 10 μL pipette tip. At 0 and 48 h, the linear wounds were observed under the microscope and quantified by Image J software [21].

Transwell assay

A 24-well Transwell chamber (354480; Corning, USA) with a 8-μm PET membrane was prepared, of which the lower chamber was loaded with medium containing 10% FBS (800 μL) and the upper chamber coated with Matrigel was covered with 10×10^4 cells. After 24 h, invaded cells were stained with crystal violet and microscopically counted in 5 fields of view [22].

Flow cytometry

Cells were rinsed with phosphate-buffered saline (P4417; Sigma-Aldrich) and resuspended in binding buffer at 1×10^6 cells/mL. After staining with Annexin V-fluorescein isothiocyanate and propidium iodide, apoptosis rate was detected by a FACS Calibur flow cytometer (BD Biosciences, NJ, USA) [23].

Detection of glycolysis

Cells (1×10^5 cells/well) were cultured in 6-well plates overnight and incubated under normoxia for 48 h. Glucose consumption was measured using glucose measurement reagent (G3293; Supelco, USA) and lactate production was determined using lactic acid measurement kit (MAK064; Sigma-Aldrich) [24].

Detection of lactate dehydrogenase (LDH)

NK cell cytotoxicity was analyzed by the LDH kit (C0016; Beyotime, Shanghai, China). Cells (1×10^4) were allowed to grow in 96-well plates for 4 h and the release of LDH was measured [25].

Tumor xenografts in nude mice

SPF-free BALB/c male nude mice (3-5 weeks old, 20 ± 5g) were reared at 25 ± 3°C with a humidity of 45-50%. The mice were randomly divided into 10 groups, each with 6 mice. Cells were resuspended in 50% Matrigel (354234; Corning, NY, USA) to 1×10^7 cells/mL, and the cell suspension (0.5 mL) was subcutaneously into the left armpit of mice which had been anesthetized with pentobarbital sodium (50 mg/kg). Tumor size was measured with a vernier caliper every 5 days, a total of 6 times. After 30 d, the mice were anesthetized with pentobarbital sodium (50 mg/kg) and euthanized to take tumors. Tumors were weighed and tumor volume (mm^3) was measured: (length × $width^2$)/2 [26].

Dual luciferase reporter gene assay

MIR4435-2HG wild-type (MIR4435-2HG-WT), MIR4435-2HG mutant (MIR4435-2HG-MUT), GPX8 wild-type (GPX8-WT) and GPX8 mutant (GPX8-MUT) fragments containing miR-582-5p binding sites were generated by GenePharma. Renilla luciferase vector pRL-TK (Promega, WI, USA), sequence fragment, and miR-582-5p mimic or miR-582-5p NC were co-transfected into PANC-1 cells for 48 h. The luciferase activity was detected by the dual luciferase system (Promega) [27].

RNA immunoprecipitation (RIP) assay

MIR4435-2HG and miR-582-5p, or miR-582-5p and GPX8 were co-transfected into PANC-1 cells, which were subsequently lysed by radio-immunoprecipitation assay lysis buffer (89901; Thermo Fisher Scientific, MA, USA) and combined with protein G agar magnetic beads containing anti-Ago2 (1:50; ab186733; Abcam, USA) or anti-IgG (1:100; sc-2025; Santa Cruz Biotechnology, Shanghai, China). The immunoprecipitates were treated with DNase I (18047019; Invitrogen) and proteinase K (4333793; Invitrogen), and RNA was recovered for reverse transcription quantitative polymerase chain reaction (RT-qPCR) [28].

RT-qPCR

RNA extraction was performed with Trizol reagent (15596018; Invitrogen). For MIR4435-2HG, GPX8 and MICA/B, reverse transcription was conducted using PrimeScript RT-PCR kit (RR014B; Takara, Kyoto, Japan), while for miR-582-5p, cDNA was assessed after treatment using TaqMan™ Advanced miRNA kit (A28007; Applied Biosystems, CA, USA). Quantitative PCR was implemented with miScript SYBR Green PCR kit (218076; Qiagen, Germany) in the ABI 7500 system. Data assessment was conducted with $2^{-\Delta\Delta Cq}$ method, employing U6 and glyceraldehyde-3-phosphate dehydrogenase (GAPDH) as internal references. The primer sequences are shown in Table 1.

Table 1
Primer sequences

Primers	Forward (5’→3’)	Reverse (5’→3’)
MIR4435-2HG	CGGAGCATGGAACTCGACA	CAAGTCTCACACATCCGGG
miR-582-5p	ATCCCTAGCTTCAACGTG	CGTTACAATTGCTAGC
GPX8	GTTTCACTAGTTGTAAACGTGGC	CGATTCTCCAAAACTGATTGCAGG
MICA	CCTTGGCCATGAACGTCAGG	CCTCTGAGGCCTCGCTGCG
MICB	CTGCTGTTTCTGGCCGTC	ACAGATCCATCCTGGGACAG
U6	CTCGCTTTCGGCAGCACA	AACGCTTTCACGAATTTGCGT
GAPDH	GAGTCAACGGATTTGGTCGT	GATCTCGCTCCTGGAAGATG

Western blot assay

Tissues or cells were lysed by 1% protease and phosphatase inhibitor, and protein concentration was detected with Pierce^{TM} BCA kit (23225; Thermo Fisher Scientific). The separated protein by sodium dodecyl sulphate polyacrylamide gel electrophoresis was transferred to a polyvinylidene fluoride membrane (FFP24; Beyotime), blocked with 5% skim milk, incubated with primary antibodies GAPDH (1:500; ab8245), GPX8 (1:500; ab183664), MICA/B (1:1000; ab222098, all from Abcam) and with the secondary antibody IgG (1:1000; ab222098). Finally, the bands were observed by enhanced chemiluminescence reagent (GE Healthcare, USA) [29].

Statistical analysis

SPSS 22.0 software (IBM, NY, USA) was applied for statistical analysis. Each experiment was repeated 3 times. Data were displayed as mean ± standard deviation and assessed by t-test or one-way analysis of variance (ANOVA) and Tukey's post-hoc test. Chi-square test and Kaplan-Meier analysis were adopted to determine the relationship between MIR4435-2HG expression and patients’ pathological features and survival, respectively. Pearson test was allowed to evaluate the correlation of MIR4435-2HG, miR-582-5p and GPX8. $P < 0.05$ presented statistical significance.

Results

Negative correlation between MIR4435-2HG expression and patients’ prognosis in PC

MIR4435-2HG suppression can inhibit cancer cell development [8, 30]. In PC, MIR4435-2HG expression was determined in clinical tissues and cells, and the outcomes reflected that MIR4435-2HG was excessively expressed in cancer tissues (Fig. 1A) and cell lines (Fig. 1B). PANC-1 cells had the most

obvious difference from hTERT-HPNE cells in the level of MIR4435-2HGs, so it was used for subsequent cell experiments.

Depending on the median value of MIR4435-2HG expression, PC cases were allocated to high expression group (n = 48) and low expression group (n = 48). Chi-square test found that MIR4435-2HG expression was correlated with tumor size, lymph node metastasis (LNM), tumor node metastasis (TNM) staging, and tumor differentiation (Table 2). Kaplan-Meier analysis showed that MIR4435-2HG high expression indicated shortened overall survival of PC patients (Fig. 1C).

Table 2
Relationship between MIR4435-2HG expression and clinicopathological characteristics of patients with PC

Parameters	Cases	MIR4435-2HG expression		*P* value
		High (n = 48)	Low (n = 48)	
Age (years)				0.2944
< 60	59	32	27	
≥ 60	37	16	21	
Gender				0.289
Male	61	33	28	
Female	35	15	20	
Tumor size (cm)				0.0136
< 2	54	21	33	
≥ 2	42	27	15	
Lymph nodes metastasis				0.0411
Negative	27	9	18	
Positive	69	39	30	
TNM stage				0.0114
I-II	36	12	24	
III-IV	60	36	24	
Tumor differentiation				0.0123
Well	12	3	9	
Moderate	34	13	21	
Poor	50	32	18	

MIR4435-2HG inhibition restrains growth, glycolysis and immunity of PC cells

si-NC and si-MIR4435-2HG were respectively transfected into PANC-1 cells, and the transfection efficiency was verified by RT-qPCR (Fig. 2A). In CCK-8 and colony formation assay, scratch test, Transwell assay, flow cytometry, it was discovered that silencing MIR4435-2HG inhibited proliferation (Fig. 2B, C), migration and invasion (Fig. 2D, E), augmented apoptosis and reduced survival rate of PANC-1 cells (Fig. 2F).

Because cancer cells have more material and energy requirements, the level of glycolysis increases, which is manifested in the increase of glucose uptake and lactate production [31]. Therefore, by testing the glucose consumption and lactate production, it was captured that lowering MIR4435-2HG expression reduced glycolysis and hindered cancer cells from obtaining energy (Fig. 2G).

LDH is not only related to glycolysis pathway, but can also promote tumor immunity by changing tumor microcircles. High LDH predicts the reduction of NK cytotoxicity [32]. MICA and MICB are ligands on the tumor surface that could promote NK cytotoxicity. Tumor immunity is usually related to the shedding of MIC on the cell membrane [33]. Detection of LDH, MICA and MICB found that after interference with MIR4435-2HG, NK cytotoxicity, and MICA/B expression were enhanced (Fig. 2H, I).

Tumor formation in nude mice displayed that PANC-1 cells carrying silenced MIR4435-2HG had inhibited ability to increase tumor volume and weight (Fig. 2J, K).

Binding of MIR4435-2HG to miR-582-5p

miR-582-5p can inhibit the progression of colorectal cancer (CRC) [34]. In PC, it was experimentally determined that miR-582-5p expression was low in cancer tissues and cell lines (Fig. 3A, B). The specific molecular relationship between MIR4435-2HG and miR-582-5p was verified through StarBase website (http://starbase.sysu.edu.cn), and the search results showed the possible binding sites between MIR4435-2HG and miR-582-5p (Fig. 3C). Immediately afterwards, dual luciferase reporter experiment and RIP experiment further verified the molecular relationship between them. The results unraveled that in the presence of mimic-miR-582-5p, the luciferase activity of MIR4435-2HG-WT was inhibited (Fig. 3D); Ago2 treatment increased the level of MIR4435-2HG and miR-582-5p enrichment (Fig. 3E).

In addition, Pearson test analyzed the correlation between MIR-4435-2HG and miR-582-5p and found that the two were negatively correlated (Fig. 3F). miR-582-5p levels were assessed to decrease in cells stably transfected with si-MIR4435-2HG (Fig. 3G).

miR-582-5p elevation hinders the malignant behaviors of PC cells

mimic-NC and mimic-miR-582-5p were transfected into PANC-1 cells respectively, and the transfection efficiency was verified (Fig. 4A). By evaluation of cell functions, it was noticed that PANC-1 cells

expressing elevated miR-582-5p exhibited cell growth inhibition, including repressed proliferation, migration and invasion, along with enhanced apoptosis (Fig. 4B-F), as well as decreased glycolysis (Fig. 4G), promoted NK cytotoxicity and elevated MICA/B expression (Fig. 4H, I).

In vivo, the ability of PANC-1 cells to promote tumor growth was restrained by up-regulated miR-582-5p, causing reduced tumor volume and weight (Fig. 4J, K).

Targeting relation between miR-582-5p and GPX8

GPX8 knockdown can effectively inhibit the growth of tumors [35]. Through RT-qPCR and Western blot, GPX8 mRNA and protein levels were discovered to be increased in cancer tissues and cell lines (Fig. 5A-D).

On the TargetScan website (http://www.targetscan.org/), it was search that there was a targeting relationship between miR-582-5p and GPX8 (Fig. 5E). Similarly, dual luciferase report experiment and RIP experiment exhibited that luciferase activity of GPX8-WT co-transfected with mimic-miR-582-5p was inhibited (Fig. 5F) and miR-582-5p and GPX8 levels were induced by Ago2 treatment (Fig. 5G).

Pearson tested found that GPX8 was positively correlated with MIR4435-2HG and negatively correlated with miR-582-5p in cancer tissues (Fig. 5H) while RT-qPCR and Western blot proved that GPX8 mRNA and protein levels were inhibited in PANC-1 cells after stable transfection with si-MIR4435-2HG or mimic-miR-582-5p (Fig. 5I-L).

GPX8 knockdown impedes the biological functions of PC cells

For clarifying GPX8's effect on PC, sh-NC and sh-GPX8 were transfected into PANC-1 cells, and the transfection results were checked by RT-qPCR and Western blot (Fig. 6A, B). Afterwards, it was further analyzed that GPX8 depletion in PANC-1 cells blocked cell growth, prevented cells from obtaining energy for glycolysis, improved NK cytotoxicity (Fig. 6C-J). *In vivo* results further confirmed the tumor suppressor effect of knocked down GPX8 in PC (Fig. 6K, L).

miR-582-5p inhibition or GPX8 overexpression reverses the effect of silenced MIR4435-2HG on inhibiting PC development

Finally, rescue experiments were set up to verify that MIR4435-2HG can mediate GPX8 through miR-582-5p to affect PC progression. Similarly, we verified the transfection efficiency of the cells by RT-qPCR and Western blot (Fig. 7A, B). Subsequently, it was disclosed that both miR-582-5p down-regulation and GPX8 up-regulation can reverse the inhibitory effect of silenced MIR4435-2HG on PANC-1 cell growth, glycolysis and immunity (Fig. 7C-L).

Discussion

PC remains a deadly disease with relatively low survival rate. Through an exploration of PC-related molecular mechanism, it was confirmed that silencing MIR4435-2HG hindered growth, glycolysis and tumor immunity of PC cells through serving as a decoy of miR-582-5p to down-regulate GPX8 (Figure 8).

Initially, our report realized that MIR4435-2HG was excessively expressed in cancer tissues of PC patients, and was correlated with tumor size, LNM, TNM stage, tumor differentiation and survival time of patients. Next, using the PC cell line, PANC-1, it was proved that silencing MIR4435-2HG enhanced proliferation, wound healing and invasion, and decreased cell apoptosis rate *in vitro*, and repressed tumor formation *in vivo*. Accordingly, a prediction analysis has demonstrated that the higher the MIR4435-2HG expression, the poorer the overall survival of patients with CRC [36]. In the case of GC, the association has been found between high MIR4435-2HG expression and patients' tumor stage, and the promoting role of MIR4435-2HG is reflected to augment aggressiveness of GC cells *in vitro* and *in vivo* [8]. As to hepatocellular carcinoma, MIR4435-2HG expression maintains a high level which is related to tumor size, and moreover, MIR4435-2HG overexpression triggers proliferation of cancer cells [37]. Consistent with this, a report of Haiyun Q *et al.* offers explanation that enriched MIR4435-2HG presents a negative correlation with LNM of patients with lung cancer, and cancer cells inhibiting MIR4435-2HG are characterized by impaired proliferation and invasion capacities [9]. Also, MIR4435-2HG down-regulation could reduce glucose consumption and lactate production, as well as increase cytotoxicity and levels of MICA and MICB, thereby inhibiting glycolysis and tumor immunity. As far as we know, the actual role of MIR4435-2HG in tumor cell glycolysis and immunity has rarely been described, which represents the innovative concept of our research.

Afterwards, miR-582-5p which was lowly expressed in PC tissues and cell lines, was discovered to be negatively regulated by MIR4435-2HG. By gene expression regulation, the tumor suppressor role of miR-582-5p was reflected in restraining cell outgrowth *in vitro* and *in vivo*, preventing glycolysis and reducing tumor immunity. On the other hand, miR-582-5p inhibition decelerated MIR4435-2HG silencing-mediated PC cell development. In fact, suppressed levels of miR-582-5p have been detected in NSCLC, and mechanistically, enforced levels of miR-582-5p in tumor cells indicate obstacles for cell growth [38]. Besides, our study results are supported by the report of Jin Y *et al*. which proves that elevating miR-582-5p expression in GC cells utmost weakens the proliferative property and strengthens apoptosis [39]. In particular, lowly expressed miR-582-5p has been once examined in human endometrial cancer, and treatment with restored miR-582-5p in tumor cells accounts for proliferation blockade and apoptosis promotion [40]. In salivary adenoid cystic carcinoma cells expressing up-regulated miR-582-5p, it could be noticed that the malignant phenotypes are all suppressed *in vitro*, and the contribution of miR-582-5p is further verified *in vivo* [41]. In an article related to bladder cancer, reduced miR-582-5p is tested in cancer samples, and miR-582-5p induction barricades cell activities *in vitro* and could even delays tumor formation *in vivo* [42]. In terms of glycolysis and immunity, miR-582-5p-related actions were seldom discussed, which shall be further probed.

In addition,our research found the targeting relation between miR-582-5p and GPX8, and further tested that GPX8 knockdown depressed the development of PC cells while GPX8 overexpression resulted in reversal of silenced MIR4435-2HG-induced effects on PC. As clinically analyzed, GPX8 high expression is an independent indicator of prognosis of breast cancer [16]. Concerning to the actual function of GPX8 in cancers, Khatib A *et al*. have explained that loss of GPX8 decelerates the formation and growth rate of breast cancer tumors in mice [15]. At present, the lack of studies regarding to GPX8-regulated glycolysis and immunity still awaits for deep analysis.

Shortly, our report supports that depleting of MIR4435-2HG elevates miR-582-5p and reduces GPX8 expression, so as to preventing cell growth, glycolysis and tumor immunity in PC. Our study analysis may offer a new niche for developing targeted therapy for PC. But, the downstream and upstream mechanisms of MIR4435-2HG/miR-582-5p/GPX8 axis in PC were not explored, which is the limitation of our research.

Declarations

Funding

none

Ethics approval and consent to participate

The study was approved by the committee of West China Hospital of Sichuan University, and all subjects had signed a written consent form. Animal treatments were processed in coincidence with Animal Care and Use Guidelines of Animal Ethic Committee in West China Hospital of Sichuan University.

Conflict of interest

The Authors declare no conflicts of interest directly related to the contents of this article.

Consent for publication

Not applicable

Availability of data and material

Not applicable

Authors' contributions

Weiming Hu contributed to study design, Huimin Lu andd Mao Li contributed to manuscript editing, Dujiang Yang, Zhenlu Li contributed to experimental studies, Chao Yue, Jiafan Song and Xing Wang contributed to data analysis.

All authors read and approved the final manuscript.

Acknowledgement

We thank the associate editor and the reviewers for their useful feedback that improved this paper.

References

1. Vincent, A., et al., *Pancreatic cancer.* Lancet, 2011. 378(9791): p. 607-20.
2. Ilic, M. and I. Ilic, *Epidemiology of pancreatic cancer.* World J Gastroenterol, 2016. 22(44): p. 9694-9705.
3. Goral, V., *Pancreatic Cancer: Pathogenesis and Diagnosis.* Asian Pac J Cancer Prev, 2015. 16(14): p. 5619-24.
4. Tempero, M.A., *NCCN Guidelines Updates: Pancreatic Cancer.* J Natl Compr Canc Netw, 2019. 17(5.5): p. 603-605.
5. Huang, X., et al., *LncRNAs in pancreatic cancer.* Oncotarget, 2016. 7(35): p. 57379-57390.
6. Sun, J., et al., *Upregulation of LncRNA PVT1 Facilitates Pancreatic Ductal Adenocarcinoma Cell Progression and Glycolysis by Regulating MiR-519d-3p and HIF-1A.* J Cancer, 2020. 11(9): p. 2572-2579.
7. Qi, C., et al., *Long non-coding RNA MACC1-AS1 promoted pancreatic carcinoma progression through activation of PAX8/NOTCH1 signaling pathway.* J Exp Clin Cancer Res, 2019. 38(1): p. 344.
8. Wang, H., et al., *LncRNA MIR4435-2HG targets desmoplakin and promotes growth and metastasis of gastric cancer by activating Wnt/beta-catenin signaling.* Aging (Albany NY), 2019. 11(17): p. 6657-6673.
9. Qian, H., et al., *The lncRNA MIR4435-2HG promotes lung cancer progression by activating beta-catenin signalling.* J Mol Med (Berl), 2018. 96(8): p. 753-764.
10. Bhan, A., M. Soleimani, and S.S. Mandal, *Long Noncoding RNA and Cancer: A New Paradigm.* Cancer Res, 2017. 77(15): p. 3965-3981.
11. Huang, S., et al., *miR-582-3p and miR-582-5p Suppress Prostate Cancer Metastasis to Bone by Repressing TGF-beta Signaling.* Mol Ther Nucleic Acids, 2019. 16: p. 91-104.
12. Liu, J., et al., *MicroRNA-582-5p suppresses non-small cell lung cancer cells growth and invasion via downregulating NOTCH1.* PLoS One, 2019. 14(6): p. e0217652.
13. Liu, K., et al., *Distinct prognostic values of mRNA expression of glutathione peroxidases in non-small cell lung cancer.* Cancer Manag Res, 2018. 10: p. 2997-3005.
14. Brigelius-Flohe, R. and M. Maiorino, *Glutathione peroxidases.* Biochim Biophys Acta, 2013. 1830(5): p. 3289-303.
15. Khatib, A., et al., *The glutathione peroxidase 8 (GPX8)/IL-6/STAT3 axis is essential in maintaining an aggressive breast cancer phenotype.* Proc Natl Acad Sci U S A, 2020. 117(35): p. 21420-21431.
16. Zhang, X., et al., *Glutathione Peroxidase 8 as a Prognostic Biomarker of Gastric Cancer: An Analysis of The Cancer Genome Atlas (TCGA) Data.* Med Sci Monit, 2020. 26: p. e921775.

17. Wang, A., et al., *ANLN-induced EZH2 upregulation promotes pancreatic cancer progression by mediating miR-218-5p/LASP1 signaling axis.* J Exp Clin Cancer Res, 2019. 38(1): p. 347.
18. Sun, Y., et al., *Transgelin-2 is a novel target of KRAS-ERK signaling involved in the development of pancreatic cancer.* J Exp Clin Cancer Res, 2018. 37(1): p. 166.
19. Lei, S., et al., *Long noncoding RNA 00976 promotes pancreatic cancer progression through OTUD7B by sponging miR-137 involving EGFR/MAPK pathway.* J Exp Clin Cancer Res, 2019. 38(1): p. 470.
20. Wang, G., et al., *Long non-coding RNA CRNDE sponges miR-384 to promote proliferation and metastasis of pancreatic cancer cells through upregulating IRS1.* Cell Prolif, 2017. 50(6).
21. Fang, C., et al., *microRNA-193a stimulates pancreatic cancer cell repopulation and metastasis through modulating TGF-beta2/TGF-betaRIII signalings.* J Exp Clin Cancer Res, 2018. 37(1): p. 25.
22. Liang, C., et al., *MiR-29a, targeting caveolin 2 expression, is responsible for limitation of pancreatic cancer metastasis in patients with normal level of serum CA125.* Int J Cancer, 2018. 143(11): p. 2919-2931.
23. Zhao, G., et al., *miR-148b functions as a tumor suppressor in pancreatic cancer by targeting AMPKalpha1.* Mol Cancer Ther, 2013. 12(1): p. 83-93.
24. Ren, S., et al., *Knockdown of circDENND4C inhibits glycolysis, migration and invasion by up-regulating miR-200b/c in breast cancer under hypoxia.* J Exp Clin Cancer Res, 2019. 38(1): p. 388.
25. Duan, Q., et al., *High glucose promotes pancreatic cancer cells to escape from immune surveillance via AMPK-Bmi1-GATA2-MICA/B pathway.* J Exp Clin Cancer Res, 2019. 38(1): p. 192.
26. Wu, X.B., et al., *Cross-talk among AFAP1-AS1, ACVR1 and microRNA-384 regulates the stemness of pancreatic cancer cells and tumorigenicity in nude mice.* J Exp Clin Cancer Res, 2019. 38(1): p. 107.
27. Meng, Q., et al., *A miR-146a-5p/TRAF6/NF-kB p65 axis regulates pancreatic cancer chemoresistance: functional validation and clinical significance.* Theranostics, 2020. 10(9): p. 3967-3979.
28. Shi, W., et al., *Long non-coding RNA LINC00346 promotes pancreatic cancer growth and gemcitabine resistance by sponging miR-188-3p to derepress BRD4 expression.* J Exp Clin Cancer Res, 2019. 38(1): p. 60.
29. Fan, P., et al., *Overexpressed histone acetyltransferase 1 regulates cancer immunity by increasing programmed death-ligand 1 expression in pancreatic cancer.* J Exp Clin Cancer Res, 2019. 38(1): p. 47.
30. Dong, X., et al., *Long Non-coding RNA MIR4435-2HG Promotes Colorectal Cancer Proliferation and Metastasis Through miR-206/YAP1 Axis.* Front Oncol, 2020. 10: p. 160.
31. Xiang, J., et al., *TCF7L2 positively regulates aerobic glycolysis via the EGLN2/HIF-1alpha axis and indicates prognosis in pancreatic cancer.* Cell Death Dis, 2018. 9(3): p. 321.
32. Fosmark, S., *[Technological standstill].* Tidsskr Nor Laegeforen, 2017. 137(14-15).
33. Shi, P., et al., *Valproic acid sensitizes pancreatic cancer cells to natural killer cell-mediated lysis by upregulating MICA and MICB via the PI3K/Akt signaling pathway.* BMC Cancer, 2014. 14: p. 370.

34. Zhang, X., et al., *Upregulation of miR-582-5p inhibits cell proliferation, cell cycle progression and invasion by targeting Rab27a in human colorectal carcinoma.* Cancer Gene Ther, 2015. 22(10): p. 475-80.
35. Chen, H., et al., *GPX8 is transcriptionally regulated by FOXC1 and promotes the growth of gastric cancer cells through activating the Wnt signaling pathway.* Cancer Cell Int, 2020. 20(1): p. 596.
36. Ouyang, W., et al., *LncRNA MIR4435-2HG predicts poor prognosis in patients with colorectal cancer.* PeerJ, 2019. 7: p. e6683.
37. Kong, Q., et al., *The lncRNA MIR4435-2HG is upregulated in hepatocellular carcinoma and promotes cancer cell proliferation by upregulating miRNA-487a.* Cell Mol Biol Lett, 2019. 24: p. 26.
38. Wang, L.L. and M. Zhang, *miR-582-5p is a potential prognostic marker in human non-small cell lung cancer and functions as a tumor suppressor by targeting MAP3K2.* Eur Rev Med Pharmacol Sci, 2018. 22(22): p. 7760-7767.
39. Jin, Y., et al., *MicroRNA-582-5p suppressed gastric cancer cell proliferation via targeting AKT3.* Eur Rev Med Pharmacol Sci, 2017. 21(22): p. 5112-5120.
40. Li, L. and L. Ma, *Upregulation of miR-582-5p regulates cell proliferation and apoptosis by targeting AKT3 in human endometrial carcinoma.* Saudi J Biol Sci, 2018. 25(5): p. 965-970.
41. Wang, W.W., et al., *miR-582-5p inhibits invasion and migration of salivary adenoid cystic carcinoma cells by targeting FOXC1.* Jpn J Clin Oncol, 2017. 47(8): p. 690-698.
42. Uchino, K., et al., *Therapeutic effects of microRNA-582-5p and -3p on the inhibition of bladder cancer progression.* Mol Ther, 2013. 21(3): p. 610-9.

Figures

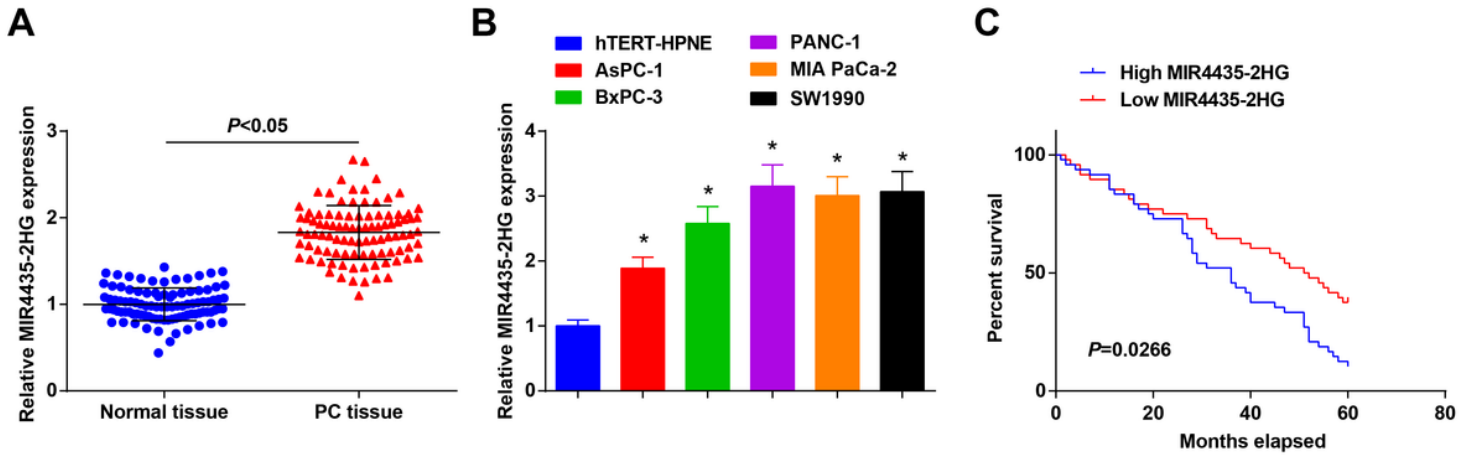

Figure 1

Negative correlation between MIR4435-2HG expression and patients' prognosis in PC. A. MIR4435-2HG expression levels in normal tissues and PC tissues, B. MIR4435-2HG expression levels in hTERT-HPNE and PC cell lines, C. Relationship between MIR4435-2HG expression levels and survival rate of PC

patients. Measurement data were expressed as mean ± standard deviation,* P < 0.05 vs hTERT-HPNE cells.

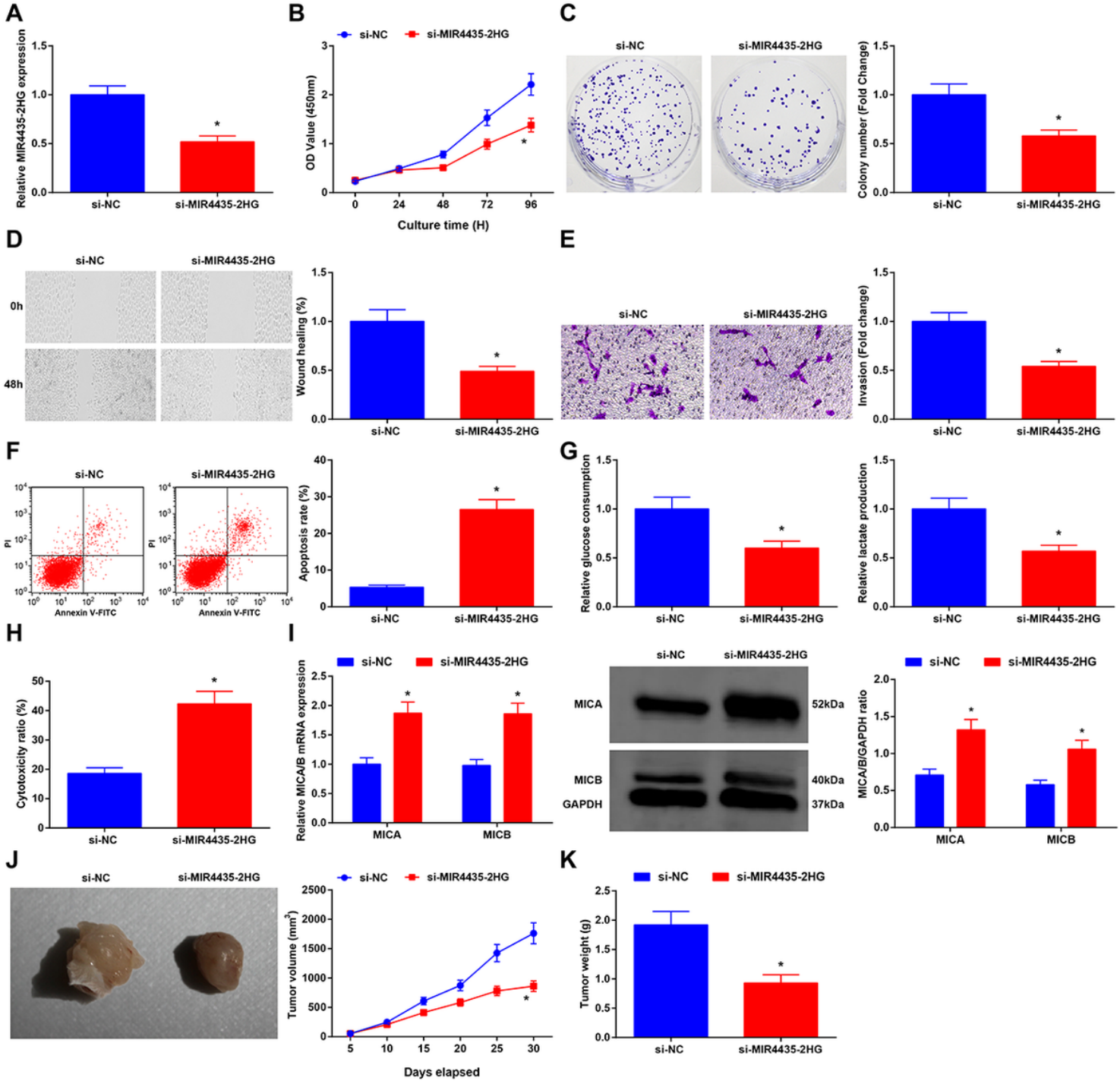

Figure 2

MIR4435-2HG inhibition restrains growth, glycolysis and immunity of PC cells. A. MIR4435-2HG mRNA expression in PANC-1 after transfection, B-C. Proliferation of PANC-1 cells after silencing MIR4435-2HG, D. Migration ability of PANC-1 cells after silencing MIR4435-2HG, E. Invasion ability of PANC-1 cells after silencing MIR4435-2HG, F. Apoptosis of PANC-1 cells after silencing MIR4435-2HG, G. Glucose consumption and lactate production in PANC-1 cells after silencing MIR4435-2HG, H. Cytotoxicity of

PANC-1 cells after silencing MIR4435-2HG, I. MICA/B expression expression in PANC-1 cells after silencing MIR4435-2HG, J-K. Tumor volume and weight in nude mice. Measurement data were expressed as mean ± standard deviation,* P < 0.05 vs the si-NC group.

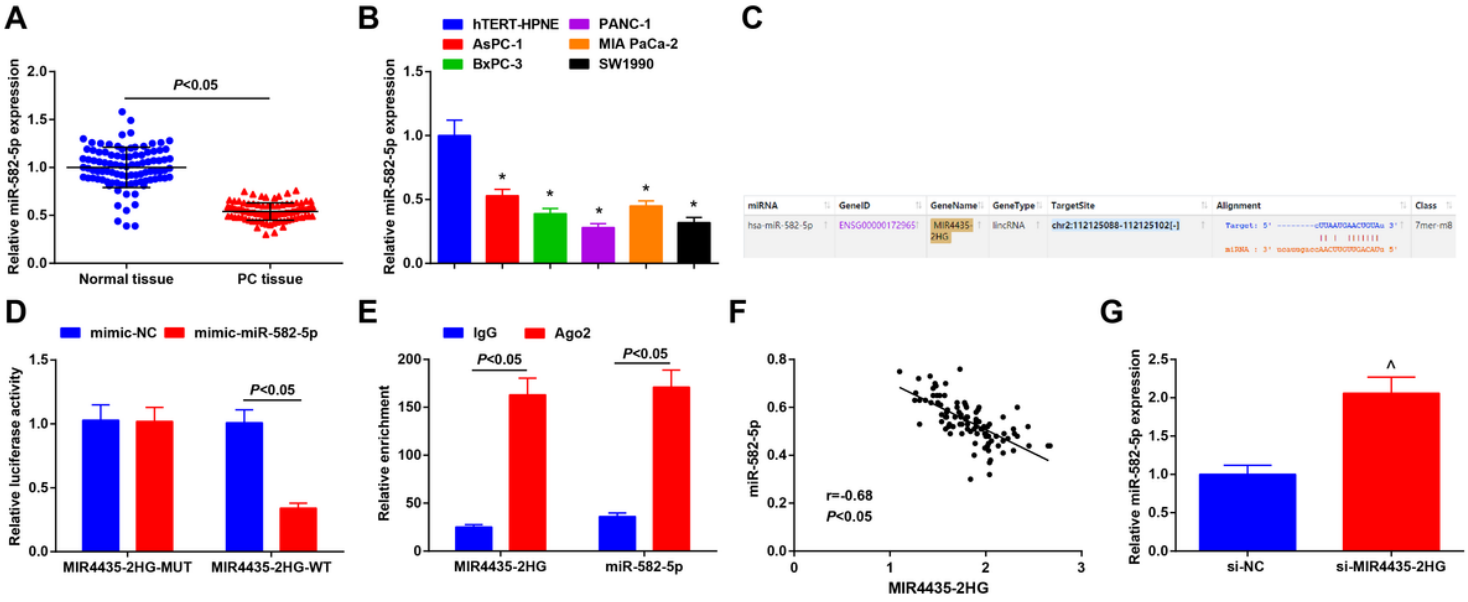

Figure 3

Binding of MIR4435-2HG to miR-582-5p. A. miR-582-5p expression in normal tissues and PC tissues, B. miR-582-5p expression in hTERT-HPNE and PC cell lines, C. Binding site between MIR4435-2HG and miR-582-5p on StarBase website, D. Luciferase activity of luciferase reporters, E. Enrichment level of MIR4435-2HG and miR-582-5p, F. Pearson correlation analysis of MIR4435-2HG and miR-582-5p levels, G. miR-582-5p expression in PANC-1 cells after silencing MIR4435-2HG. Measurement data were expressed as mean ± standard deviation,* P < 0.05 vs hTERT-HPNE cells, ^ P < 0.05 vs the si-NC group.

Figure 4

miR-582-5p elevation hinders the behaviors of PC cells. A. miR-582-5p expression in PANC-1 cells after transfection, B-C. Proliferation of PANC-1 cells after restoring miR-582-5p, D. Migration ability of PANC-1 cells after restoring miR-582-5p, E. Invasion ability of PANC-1 cells after restoring miR-582-5p, F. Apoptosis of PANC-1 cells after restoring miR-582-5p, G. Glucose consumption and lactate production in PANC-1 cells after restoring miR-582-5p, H. Cytotoxicity level of PANC-1 cells after restoring miR-582-5p, I. MICA/B expression expression in PANC-1 cells after restoring miR-582-5p, J-K. Tumor volume and weight in nude mice. Measurement data were expressed as mean ± standard deviation,* P < 0.05 vs the mimic-NC group.

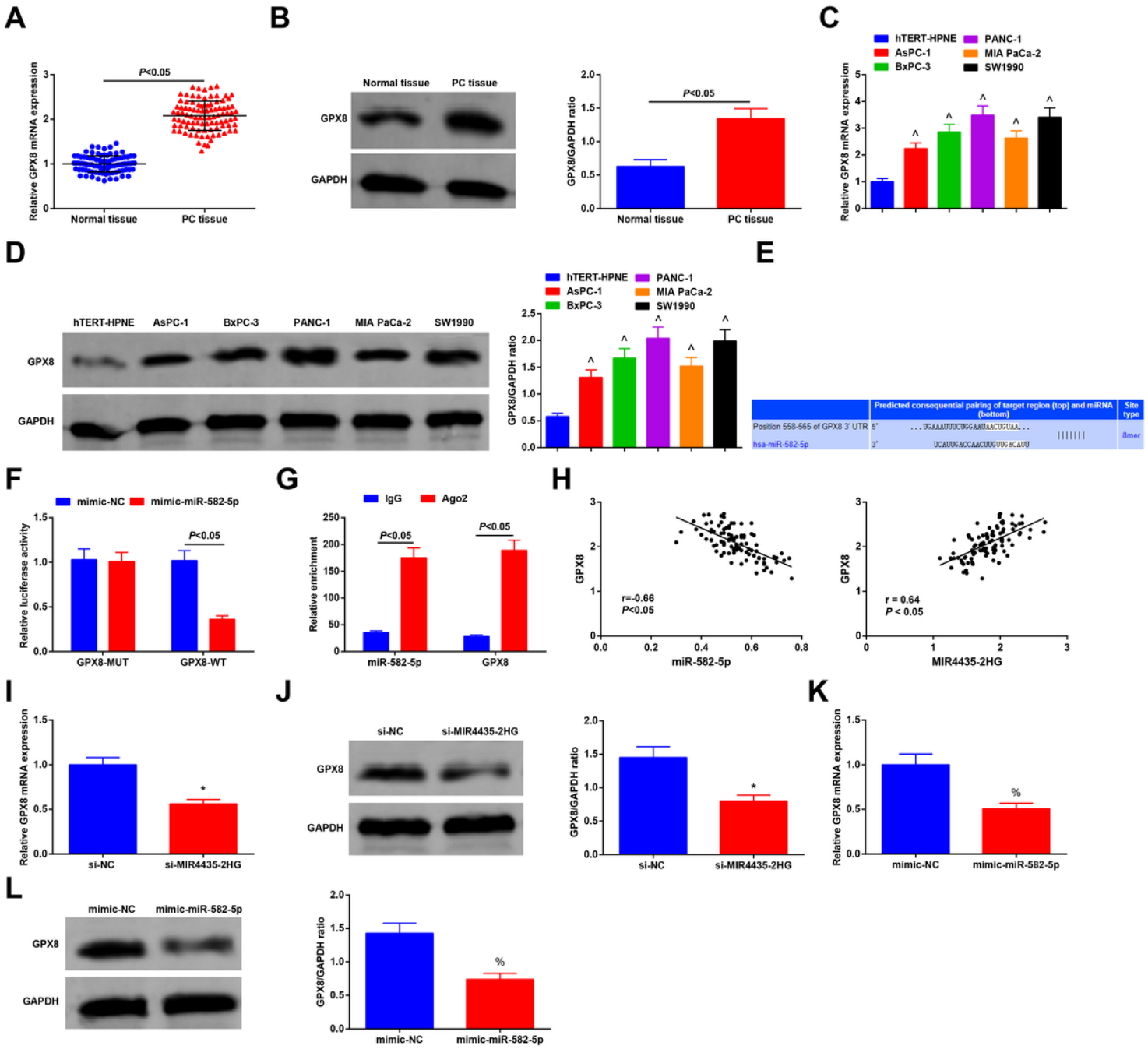

Figure 5

Targeting relation between miR-582-5p and GPX8. A-B. GPX8 mRNA and protein expression in normal tissues and PC tissues, C-D. GPX8 mRNA and protein expression in hTERT-HPNE and PC cell lines, E. Targeting sites between miR-582-5p and GPX8 on TargetScan website, F. Luciferase activity of GPX8-WT/MUT, G. enrichment level of miR-582-5p and GPX8, H. Pearson correlation analysis of GPX8 with miR-582-5p or MIR4435-2HG levels, I-J. GPX8 mRNA and protein in PANC-1 cells after silencing MIR4435-2HG, K-L. GPX8 mRNA and protein in PANC-1 cells after restoring miR-582-5p. Measurement data were expressed as mean ± standard deviation, # P < 0.05 vs Normal tissue, ^ P < 0.05 vs hTERT-HPNE cells, * P < 0.05 vs the si-NC group, % P < 0.05 vs the mimic-NC group.

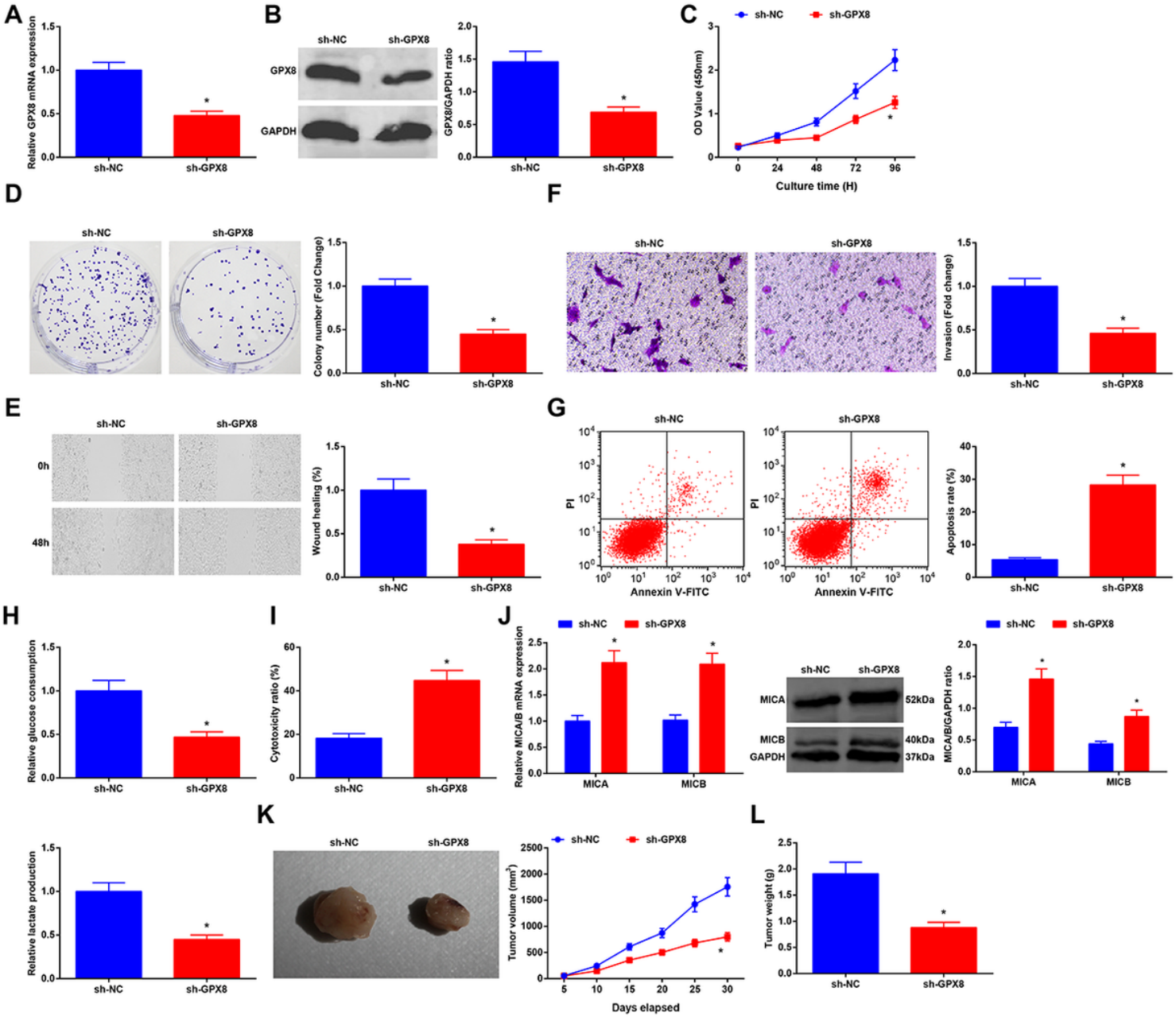

Figure 6

GPX8 knockdown impedes the biological functions of PC cells. A-B. GPX8 mRNA and protein expression in PANC-1 cells after transfection, C-D. Proliferation of PANC-1 cells after down-regulating GPX8, E. Migration ability of PANC-1 cells after down-regulating GPX8, F. Invasion ability of PANC-1 cells after down-regulating GPX8, G. Apoptosis of PANC-1 cells after down-regulating GPX8, H. Glucose consumption and lactate production of PANC-1 cells after down-regulating GPX8, I. Cytotoxicity of PANC-1 cells after down-regulating GPX8, J. MICA/B expression expression in PANC-1 cells after down-regulating GPX8, K-L. Tumor volume and weight in nude mice. Measurement data were expressed as mean ± standard deviation,* $P < 0.05$ vs the sh-NC group.

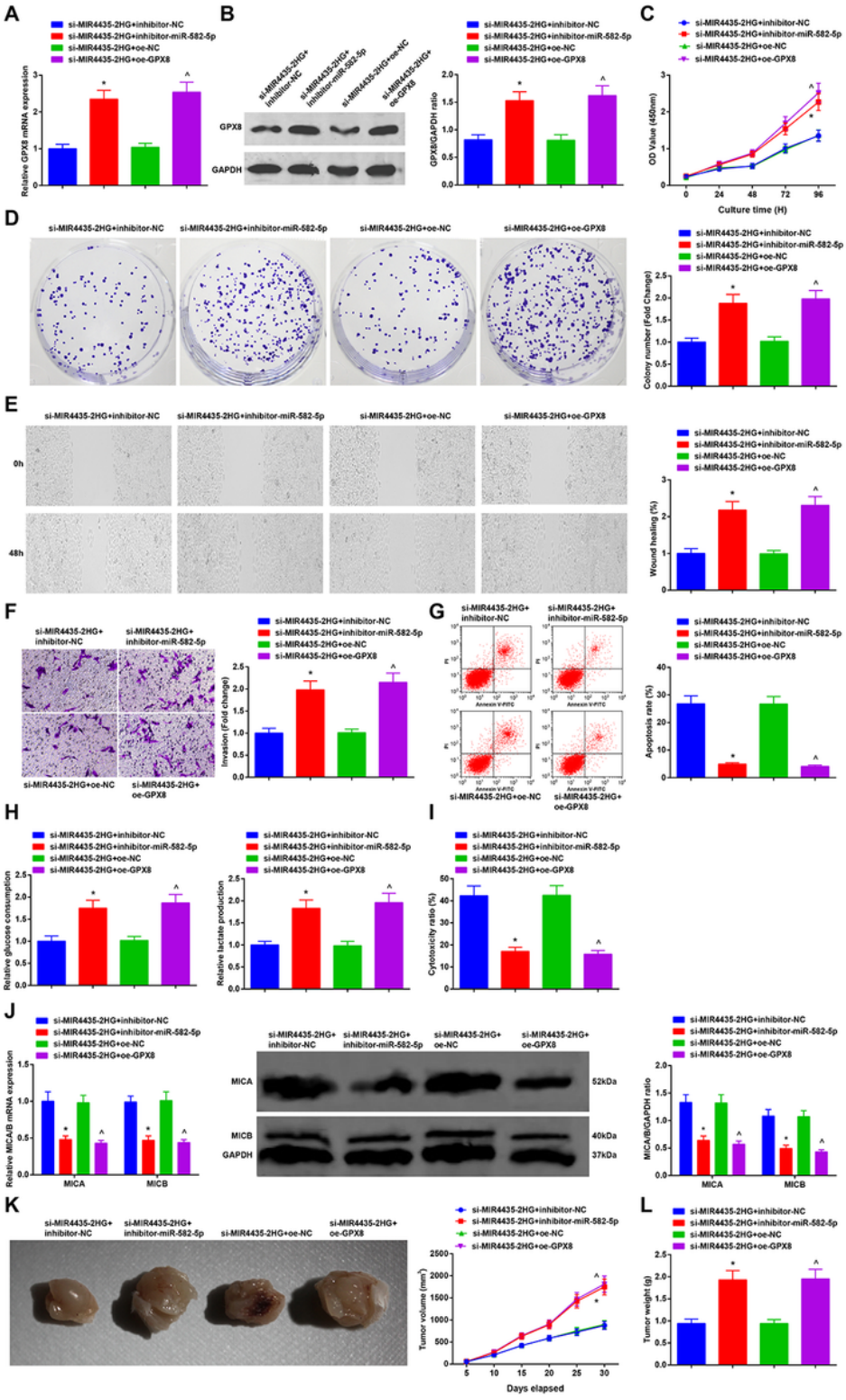

Figure 7

miR-582-5p inhibition or GPX8 overexpression reverses the effect of silenced MIR4435-2HG in inhibiting PC development. A-B. GPX8 mRNA and protein expression in PANC-1 cells after transfection, C-D. Proliferation of PANC-1 cells in rescue tests, E. Migration ability of PANC-1 cells in rescue tests, F. Invasion ability of PANC-1 cells in rescue tests, G. Apoptosis of PANC-1 cells in rescue tests, H. Glucose consumption and lactate production of PANC-1 cells in rescue tests, I. Cytotoxicity of PANC-1 cells in

rescue tests, J. MICA/B expression expression in PANC-1 cells in rescue tests, K-L. Tumor volume and weight in nude mice. Measurement data were expressed as mean ± standard deviation,* P < 0.05 vs the si-MIR4435-2HG + inhibitor-NC group, ^ P < 0.05 vs the si-MIR4435-2HG + oe-NC group.

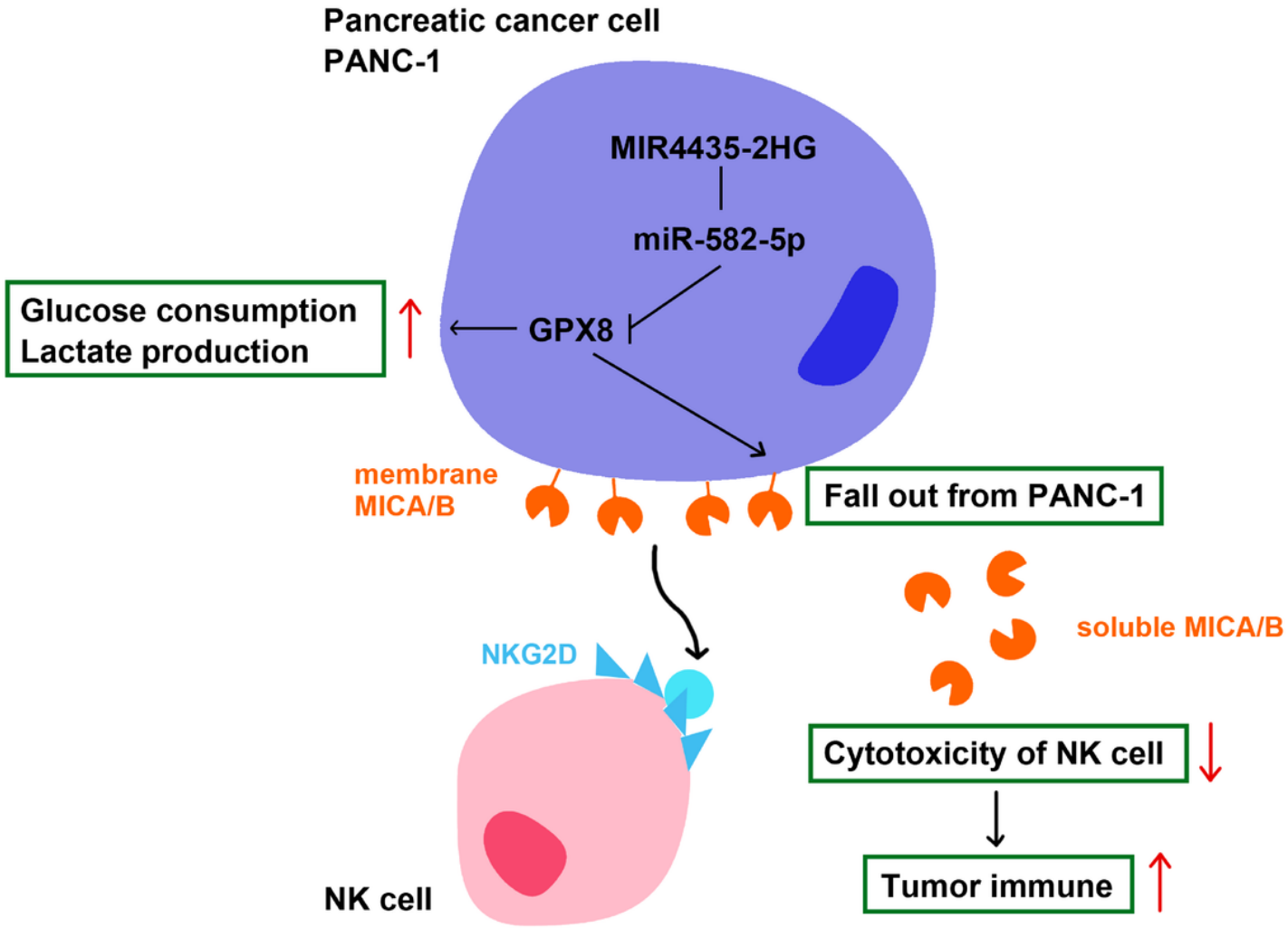

Figure 8

MIR4435-2HG promotes glycolysis and tumor immunity in PC through absorption of miR-582-5p to target GPX8.